Spin transition polymer with a large hysteresis around room temperature: optical response and electron paramagnetic resonance

1998 J. Phys.: Condens. Matter 10 7057

(http://iopscience.iop.org/0953-8984/10/31/021)

J. Phys.: Condens. Matter **10** (1998) 7057–7064. Printed in the UK PII: S0953-8984(98)93375-6

Spin transition polymer with a large hysteresis around room temperature: optical response and electron paramagnetic resonance

Christophe Cantin†, Hervé Daubric†, Janis Kliava†§, Yves Servant†, Line Sommier‡ and Olivier Kahn‡

† Centre de Physique Moléculaire Optique et Hertzienne, UMR Université Bordeaux I-CNRS 5798, 351 Cours de la Libération, 33405 Talence Cédex, France

‡ Laboratoire des Sciences Moléculaires, Institut de Chimie de la Matière Condensée de Bordeaux, UPR CNRS 9048, 33608 Pessac Cédex, France

Received 14 April 1998

Abstract. A polymer compound $[Fe(NH_2trz)_3](NO_3)_2$ has been studied by optical response and electron spin resonance (EPR) using Cu^{2+} and Mn^{2+} as dopants and paramagnetic probes. The transition between low-spin (LS) and high-spin (HS) states of Fe^{2+} ions occurs with a broad hysteresis loop around room temperature and is accompanied by a colour change from bright pink in the LS state to chalky white in the HS state. With increasing doping level the hysteresis loop narrows and shifts to lower temperatures. In the HS state of Fe^{2+} the EPR spectra of Cu^{2+} and Mn^{2+} are severely broadened by spin–spin interactions with paramagnetic HS Fe^{2+} modulated by a rapid spin–lattice relaxation of the latter ions. The EPR data give evidence of the presence of domains of the LS and HS Fe^{2+} ions in the transition region.

1. Introduction

In octahedral ligand fields transition metal ions with d^4 to d^7 configurations adopt either a high-spin (HS) or a low-spin (LS) electronic arrangement, according to whether the crystal field energy is lower or higher than the mean spin coupling energy. If the two energies are comparable, transitions between the two spin states can be brought about, e.g., by varying temperature. In many cases, particularly for ferrous compounds, bistability takes place, i.e. LS to HS and HS to LS transitions occur at different temperatures, forming a hysteresis loop. Materials in which the thermally induced spin transitions take place near room temperature are interesting in view of their possible use as molecular electronics devices, namely, for the purpose of information recording and processing. The characteristics of the spin transitions are determined to a large extent by accompanying structural transformations, so that structural analysis of spin transition materials is of primary importance [1]. Particularly well adapted to such studies is electron paramagnetic resonance (EPR) which is both a magnetic spectroscopy technique and a structure-sensitive method of analysis.

A direct EPR detection of the spin transition of ferrous ion Fe^{2+} ($3d^6$ configuration) is not possible, because at elevated temperatures Fe^{2+} produces no detectable EPR signal both in the LS ($S = 0$) *diamagnetic* state and in the HS ($S = 2$) *paramagnetic* state [2]. Yet

§ To whom correspondence should be addressed: phone (33) 556 84 61 72, fax (33) 556 84 69 70. E-mail address: jkliava@frbdx11.cribx1.u-bordeaux.fr.

0953-8984/98/317057+08$19.50

doping a ferrous matrix with small amounts of another paramagnetic ions allows *indirect* studies of the spin transitions by EPR.

In this work we report variable temperature optical response and EPR studies of a triazole-based ferrous polymeric compound $[Fe(NH_2trz)_3](NO_3)_2$ doped by Cu^{2+} ($S = 1/2$, $I = 3/2$) or Mn^{2+} ($S = 5/2$, $I = 5/2$).

2. Experimental section

Three samples of $[Fe(NH_2trz)_3](NO_3)_2$ doped respectively with 1 and 10% Cu/Fe, and 1% Mn/Fe were synthesized in powder form. The x-ray diffraction data indicate a poor crystallization of $[Fe(NH_2trz)_3](NO_3)_2$ [3, 4]. Wide angle x-rays scattering (WAXS) data suggest that the basic structure of $[Fe(NH_2trz)_3](NO_3)_2$ is that of a linear chain in which two adjacent iron atoms are triply bridged by 4-amino-1,2,4-triazole ligands (NH_2trz) through the nitrogen atoms occupying the 1 and 2 positions, see figure 1 [5].

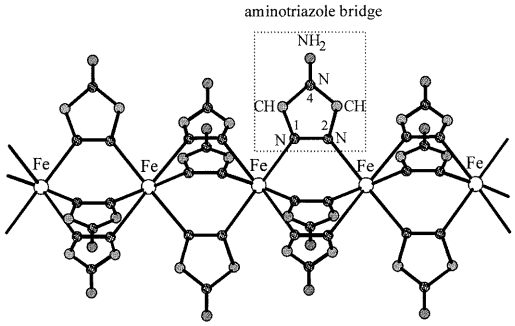

Figure 1. Structure of the polymeric compound $[Fe(NH_2trz)_3](NO_3)_2$ with NH_2trz = 4-amino-1,2,4-triazole [1].

The optical response of the samples was detected with a device described in [6].

The EPR spectra were recorded with an X-band (9.5 GHz) spectrometer (Varian) using a dual sample rectangular TE102 mode cavity; the EPR spectra of DPPH ($g_{DPPH} = 2.003\,66 \pm 0.000\,04$) and Mn^{2+} ions in MgO solid solution ($G_{MgO} = 2.0014 \pm 0.0001$, $A_{MgO} = (81.2 \pm 0.5)\ 10^{-4}\ cm^{-1}$) were used as field markers.

Computer simulations of the EPR spectra were carried out on a PC Pentium 133 MHz using a laboratory developed software.

3. Optical response results

In all the $[Fe(NH_2trz)_3](NO_3)_2$ samples the spin transition of Fe^{2+} ions is characterized by a pronounced thermochromic effect between bright pink colour in the LS state and chalky white colour in the HS state, so that the spin transition can be detected optically.

The optical response displays a spin transition with hysteresis, as shown in figure 2. The characteristic temperatures, respectively, $T_{1/2\uparrow}$ in the warming mode and $T_{1/2\downarrow}$ in the cooling mode correspond to equal numbers of LS and HS Fe^{2+} ions. Successive thermal cycles do not appreciably modify $T_{1/2\downarrow}$ but $T_{1/2\uparrow}$ is shifted towards lower temperatures and stabilizes after three cycles. The stabilized $T_{1/2}$ values are given in table 1.

It is seen that doping with copper has not much effect upon the $T_{1/2\downarrow}$ values, while the stabilized $T_{1/2\uparrow}$ values are more doping sensitive. Note that in the 10% Cu/Fe-doped

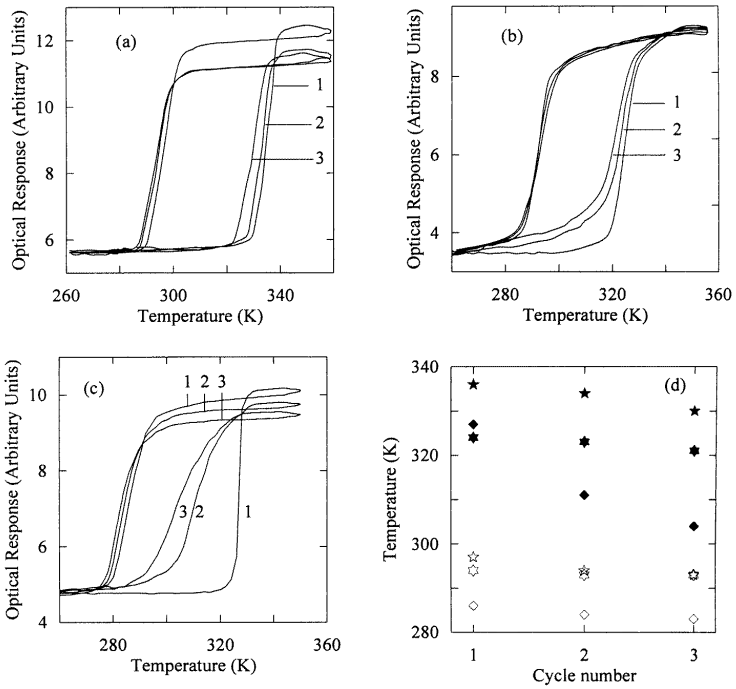

Figure 2. Optical response of the 1% Cu/Fe (a), 10% Cu/Fe (b) 0 and 1% Mn/Fe (c) samples and the characteristic spin transition temperatures in the warming (full symbols) and cooling mode (empty symbols) for the 1% Cu/Fe (★, ☆) 10% Cu/Fe (✸, ✩) and 1% Mn/Fe (⧫, ◊) samples (d). The successive thermal cycles are numbered 1, 2 and 3.

Table 1. Stabilized characteristic temperatures of the spin transition in the warming and cooling modes.

Sample	$T_{1/2\uparrow}$ (K)	$T_{1/2\downarrow}$ (K)
1% Cu/Fe	330	294
10% Cu/Fe	321	293
1% Mn/Fe	304	293

sample in comparison with the 1% Cu/Fe-doped one, the centre of the hysteresis loop is shifted from 312 to 307 K, a value near room temperature. Simultaneously, the hysteresis loop is narrowed from 36 K down to 28 K and the spin transition becomes less abrupt.

Doping the compound with manganese has a more pronounced effect upon the characteristics of the hysteresis loop which is dramatically narrowed in the course of the first three cycles, from 41 K to a stabilized value of 21 K, the latter value being considerably lower than that for the same copper-doping level.

4. EPR results

Figure 3 shows the evolution of the EPR spectra of the 1% Cu/Fe and 1% Mn/Fe samples of $[Fe(NH_2trz)_3](NO_3)_2$ in the temperature range of the spin transition. In the warming mode, as long as the temperature remains lower than $T_{1/2\uparrow}$, in the copper-doped samples an EPR spectrum of Cu^{2+} at $g_{ef} \approx 2$ is observed. Unlike in the $[Fe(Htrz)_2(trz)](BF_4)$

compound [7, 8], no EPR spectra due to Fe^{3+} ions are present. In the manganese-doped sample the EPR spectra in the LS state of Fe^{2+} ions exhibit a quadratic fine structure (QFS), in particular, a singularity at $g_{ef} \approx 4.3$ characteristic of $S = 5/2$ Mn^{2+} ions in a low-symmetry strong crystal field [9]. In the course of the LS to HS transition the EPR spectra of Cu^{2+} and Mn^{2+} gradually disappear and become unobservable when all the Fe^{2+} ions are in the HS (paramagnetic) state. In the cooling mode, as the temperature decreases below $T_{1/2\downarrow}$, the EPR spectra recover their initial shapes.

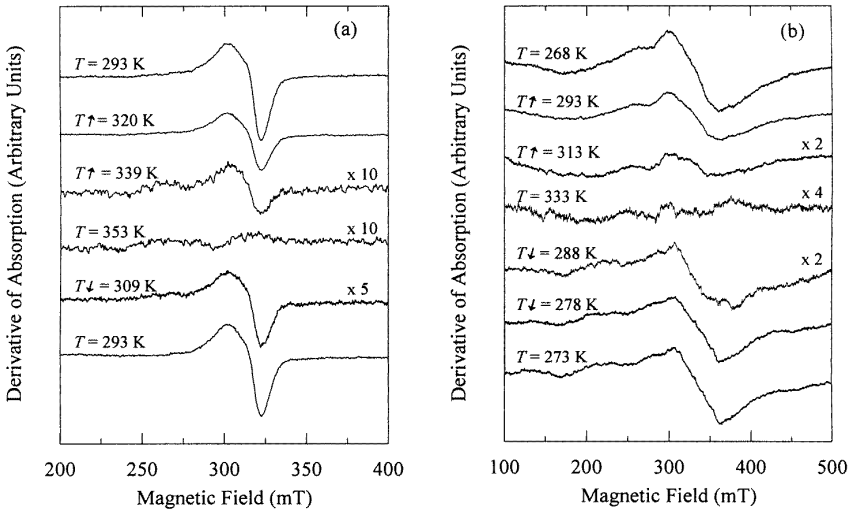

Figure 3. EPR spectra in the spin transition region in the warming ($T_{\uparrow}$) and cooling ($T_{\downarrow}$) modes for the 1% Cu/Fe (a) and 1% Mn/Fe (b) samples.

The Mn^{2+} EPR spectrum does not much change by cooling down the sample to 113 K, see figure 4. However, the resolution is somewhat improved, so that a hyperfine sextet emerges in the QFS component at $g_{ef} \approx 2.0$, with a mean splitting between the hyperfine peaks of ∼9.1 mT. Besides, a new single line appears in the central part of the $g_{ef} \approx 4.3$ component which can be assigned to traces of Fe^{3+} ions.

No modifications in the Cu^{2+} EPR spectra are observed over the range between liquid helium and liquid nitrogen temperatures. This low temperature spectrum shows a marked g-factor anisotropy and a well resolved hyperfine quadruplet in the parallel orientation of the applied magnetic field, as shown in figure 4. This spectrum can be described by the usual spin Hamiltonian

$$\mathcal{H} = \beta \boldsymbol{S} \cdot \mathbf{g} \cdot \boldsymbol{B} + \boldsymbol{S} \cdot \mathbf{A} \cdot \boldsymbol{I} \tag{1}$$

where $\mathbf{g}$ and $\mathbf{A}$ are respectively the g-tensor and the hyperfine structure tensor.

The Cu^{2+} EPR spectra have been computer simulated by means of the following relation [9]:

$$\mathcal{I}(B) = \sum_{l=1}^{2} a_l \sum_{m=-3/2}^{3/2} \int_0^{2\pi} \mathrm{d}\varphi \int_0^{\pi} \mathrm{d}\vartheta \, \sin\vartheta \, \overline{W}_m(g_x, g_y, g_z, \vartheta, \varphi) \left| \frac{\partial B_{\mathrm{rl}}}{\partial h\nu} \right| F\left(\frac{B - B_{\mathrm{rl}}}{\Delta B} \right). \tag{2}$$

The first sum takes into account the existence of the two copper isotopes, ^{63}Cu and ^{65}Cu, with natural isotopic abundances a_l of 69.1 and 30.9%, respectively. The second sum accounts for the four allowed hyperfine lines, m varying from $-3/2$ to $+3/2$. The integrals

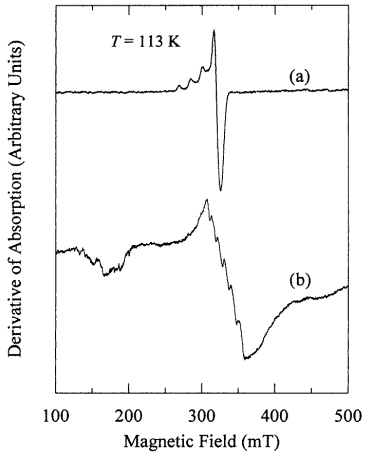

Figure 4. EPR spectra of the 1% Cu/Fe (a) and 1% Mn/Fe (b) samples at 113 K.

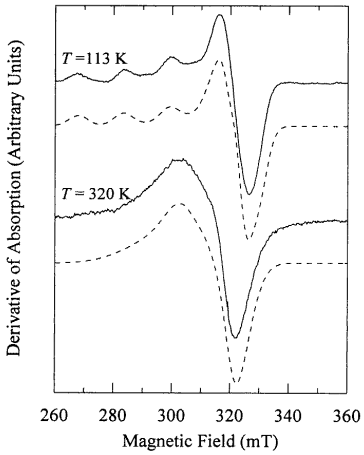

Figure 5. Computer simulations of the EPR spectrum of the 1% Cu/Fe sample at 113 K and at 320 K (after subtracting traces of the low-temperature spectrum).

over ϑ and φ take into account random orientations of paramagnetic sites with respect to the static magnetic field direction. $\overline{W}_m(g_x, g_y, g_z, \vartheta, \varphi)$ is the transition probability, B_{tl} is the resonance magnetic field, h is the Planck constant and ν is the microwave frequency of the EPR spectrometer. An orientation-dependent Gaussian lineshape function $F[(B - B_{tl})/\Delta B]$ is chosen with an orientation-dependent linewidth including different broadening mechanisms, *viz.*, disorder-caused broadening and unresolved superhyperfine splitting etc [9].

A computer fitting to the low-temperature Cu^{2+} EPR spectrum, as shown in figure 5, results in the best-fit principal values of g- and A-tensors given in table 2 (the error limits have been estimated by means of trial simulations with parameter values slightly different from the best-fit ones). These values are characteristic of an elongated octahedral environment typical of a static Jahn–Teller d^9 electronic configuration of Cu^{2+} ions. Note that the actual symmetry of Cu^{2+} sites is lower than axial.

Table 2. Best-fit magnetic parameters of Cu^{2+} ions at 113 and 320 K (the $A/\beta g$-values are given in millitesla; figures in parentheses are the standard errors in the last digit).

T (K)	g_x	g_y	g_z	$A_x/\beta g_x$	$A_y/\beta g_y$	$A_z/\beta g_z$
113	2.040 (5)	2.095 (5)	2.290 (5)	−1 (1)	0 (1)	−16.0 (3)
320	2.083 (5)	2.148 (5)	2.219 (5)	−3 (1)	−4 (1)	−10.7 (5)

At intermediate temperatures between 113 K and the onset of the spin transition the Cu^{2+} EPR spectra can be satisfactorily accounted for as weighted sums of the low-temperature spectrum and a much more isotropic spectrum which predominates at higher temperatures. This somewhat surprising finding can be explained in terms of a model based on a statistical distribution of the energy difference between the lowest and the two higher potential energy minima of the Jahn–Teller centre in a low-symmetry host site. This work is in progress now and will be published separately. The computer simulations of the high-temperature spectrum yield the magnetic parameter values quoted in table 2.

5. Discussion

5.1. Characteristics of the spin transition hysteresis loop

The optical response results show that for successive thermal cycles the transition temperatures in the cooling mode, $T_{1/2\downarrow}$, remain nearly constant while in the warming mode $T_{1/2\uparrow}$ lowers for the two first cycles and stabilizes itself after the third cycle. A similar behaviour has been observed in the static magnetic susceptibility [4] and optical response and EPR [7, 8] studies of $[Fe(Htrz)_2(trz)](BF_4)$ compound, so that it is characteristic of triazole-based compounds and not of a specific measuring technique.

The gradual narrowing of the hysteresis loop can be understood if one takes into account dilatation of the Fe^{2+} coordination polyhedra in the course of the LS to HS transition. Indeed, from the WAXS data [5] the distances between ferrous ions and their nearest nitrogen neighbours are estimated as 0.201 nm in the LS state and 0.218 nm in the HS state of Fe^{2+}. One might guess that in the course of the first LS to HS transition in an as-made compound the molecular chains are re-arranged in order to accommodate themselves to the dilated coordination polyhedra of HS Fe^{2+} ions. As intermolecular forces oppose themselves to such a re-arrangement, the LS to HS transition is inhibited, which results in a higher $T_{1/2\uparrow}$ value in the first hysteresis cycle. In the course of subsequent cycles the new arrangement of the molecular chains is approximately preserved. This arrangement being better adapted to the size of the HS Fe^{2+} coordination polyhedra, the stabilized $T_{1/2\uparrow}$ values are lower than in the first hysteresis cycle.

The gradual lowering of the $T_{1/2\uparrow}$ values is less pronounced for the Cu-doped samples than for the Mn-doped one. This is probably due to the fact that the ionic radius of Cu^{2+}, 0.73 Å, has an intermediate value between those of Fe^{2+} in its two spin states, 0.61 Å in the LS state and 0.78 Å in the HS state, and is smaller than that of Mn^{2+}, 0.83 Å (see [10] for the ionic radii). Therefore, less disorder is introduced by doping the ferrous matrix with copper than with manganese, so that in the first case the arrangement of the molecular chains can be more easily re-organized in the course of the LS to HS transition. The relative stability of the $T_{1/2\downarrow}$, values can be explained by the fact that, in contrast to dilatation, contraction of the coordination polyhedra of Fe^{2+} does not require much re-organization of the molecular chains.

One can see from figure 2 that doping not only reduces the width of the hysteresis loop but also smoothes its ascending and descending sides, so that the loop becomes more rounded. These transformations can be accounted for on the basis of thermodynamic model of interacting domains which predicts this type of behaviour if the size of LS and HS domains is reduced [11]. Indeed, foreign ions inserted between the Fe^{2+} ions impose geometrical limits on the domain size.

5.2. Structural inferences

From an inspection of table 2 it is seen that the average g- and A-values,

$$\langle g\rangle = \tfrac{1}{3}(g_x + g_y + g_z) \text{ and } \langle A\rangle = \tfrac{1}{3}(A_x + A_y + A_z)$$

and are only slightly different at 113 K, $\langle g\rangle = 2.142$, $\langle A/\beta g\rangle = -6.02$ mT, and at 320 K, $\langle g\rangle = 2.150$, $\langle A/\beta g\rangle = -5.98$ mT, so that the spectrum transformations between the two temperatures can be accounted for by a motional averaging of the Jahn–Teller distortions of the Cu^{2+} ions.

In contrast to some other copper-doped nitrogen-containing ferrous complexes [12], in $[Fe(Htrz)_2(trz)](BF_4)$ no superhyperfine structure from the ^{14}N isotope (the nuclear spin

$I = 1$) can be resolved in the Cu^{2+} EPR spectra in the LS state of Fe^{2+} ions. However, computer simulations of these spectra show some inhomogeneous broadening, possibly due to an unresolved superhyperfine splitting.

The results of computer simulations of the Cu^{2+} EPR signal at 113 K show a less pronounced rhombic distortion in the environment of the copper ions in comparison with Cu-doped $[Fe(Htrz)_2(trz)](BF_4)$ compound [7, 8]. In $[Fe(NH_2trz)_3](NO_3)_2$ two consecutive ferrous ions are triply bridged by amino-triazole ligands, while in $[Fe(Htrz)_2(trz)](BF_4)$ one of three triazole bridges is spontaneously deprotonated [1]. This may result in a more pronounced distortion of the host sites and, consequently, in more rhombic EPR spectra of Cu^{2+} in the latter compound.

In the course of the spin transition a gradual *decrease* of the amplitudes of Cu^{2+} and Mn^{2+} EPR spectra is observed, rather than a gradual line *broadening*, see figure 3. This behaviour is indicative of a coexistence in the spin transition region of LS and HS Fe^{2+} domains. In this event, most of Cu^{2+} ions will be predominantly surrounded either with LS Fe^{2+} ions or with HS Fe^{2+} ions. In the former case their EPR signals will not be appreciably modified, whereas in the second case they will be severely broadened (beyond the possibility of observation at the X-band).

5.3. Linewidths in the HS state of Fe^{2+} ions

The number of HS Fe^{2+} ions is rapidly growing in the course of the spin transition and when all the Fe^{2+} ions are in the HS state, the EPR spectra of Cu^{2+} or Mn^{2+} are no more observed. Note that the vanishing of the hyperfine structure in the Mn^{2+} EPR spectrum at room temperature can be explained by the advent of a certain number of Fe^{2+} ions in the HS state, see the optical response data for the manganese-doped sample in figure 2.

In the vicinity of room temperature the spin–lattice relaxation of Cu^{2+} and Mn^{2+} remains very slow (if there is no cross-relaxation between these ions and the HS Fe^{2+} ions) and does not appreciably contribute to their linewidths. (We have mentioned in section 4 that the transformation of the Cu^{2+} ions between liquid nitrogen and room temperatures is due to a dynamical averaging of the Jahn–Teller distortions.)

When the Fe^{2+} ions are in their HS state, the $[Fe(NH_2trz)_3](NO_3)_2$ compound becomes an undiluted paramagnet, so that the widths of the Cu^{2+} and Mn^{2+} EPR spectra are determined by two competitive mechanisms: spin–spin interactions between these ions and paramagnetic Fe^{2+} ions and a fast spin–lattice relaxation of the latter ions.

The distances between the ferrous ions in $[Fe(NH_2trz)_3](NO_3)_2$ are relatively small, about 0.38 nm in the HS state [5]. The paramagnetic probes substituting themselves for the iron, random magnetic fields produced at the sites of Cu^{2+} or Mn^{2+} would result in severe *dipole–dipole* broadening of their EPR spectra. *Exchange* interaction between Cu^{2+} or Mn^{2+} and paramagnetic Fe^{2+} ions must also be taken into account, as the exchange integrals in similar triazole-based compounds from static magnetic susceptibility measurements are evaluated to several cm^{-1} [1]. Meanwhile, $[Fe(NH_2trz)_3](NO_3)_2$ and $[Fe(Htrz)_2(trz)](BF_4)$ have very similar structures, namely, almost identical metal-to-metal distances. Therefore, the spin–spin interactions alone would have resulted in very close linewidths in the two compounds, whereas the previous studies indicate a much less pronounced EPR spectrum broadening in $[Fe(Htrz)_2(trz)](BF_4)$ [7, 8].

Yet, the 'static' broadening of the Cu^{2+} or Mn^{2+} EPR spectra by spin–spin interactions is reduced because of its 'dynamical' *modulation* by the fast spin–lattice relaxation of Fe^{2+} ions; on the other hand, this relaxation can directly contribute to line broadening via the *cross-relaxation* mechanism [2]. In this context, we remind the reader that

in $[Fe(NH_2trz)](NO_3)_2$ the spin transition occurs around room temperature and in $[Fe(Htrz)_2(trz)](BF_4)$ some 30 K higher [7, 8]. The cross-relaxation rate increasing rapidly with temperature, its contribution would lead to less spectrum broadening in the first compound than in the second one, in disagreement with the experimental results. In contrast, at higher temperatures the spin–lattice relaxation of Fe^{2+} will result in a more important modulation of the spin–spin broadening, hence, to narrower EPR spectra, conforming to what is actually observed in the spin transition triazole compounds.

6. Conclusion

In $[Fe(NH_2trz)_3](NO_3)_2$ the spin transition temperatures closely approach room temperature and large and abrupt hysteresis loops are observed, making this compound interesting for technical applications. Doping ferrous spin transition compounds with paramagnetic probes makes possible their study by the EPR technique. Besides, doping is of practical interest, since it allows to fine-tune the spin transition temperatures and the width of the hysteresis loop with respect to room temperature.

The LS to HS transition of Fe^{2+} ions manifests itself in the optical response by a spectacular colour change and in the EPR by a severe broadening of spectra of both the paramagnetic probes Cu^{2+} or Mn^{2+}. This broadening is accounted for by a dynamical modulation of the spin–spin interactions between the paramagnetic probes and paramagnetic Fe^{2+} ions caused by a fast spin–lattice relaxation of the latter. The EPR spectrum transformations in the transition region indicate the presence of domains of LS and HS Fe^{2+} ions.

References

[1] Kahn O and Codjovi E 1996 *Phil. Trans. R. Soc.* A **354** 359
[2] Abragam A and Bleaney B 1970 *Electron Paramagnetic Resonance of Transition Ions* (Oxford: Clarendon)
[3] Lavreneva L G, Ikorskii V N, Varnek V A, Oglezneva I M and Larionov S V 1990 *Koord. Khim.* **16** 654
[4] Kröber J *et al* 1994 *Chem. Mater.* **6** 1404
[5] Verelst M, Sommier L, Lecante P, Mosset A and Kahn O 1998 *Chem. Mater.* **10** 980
[6] Codjovi E, Sommier L, Kahn O and Jay C 1996 *New J. Chem.* **20** 503
[7] Cantin C, Kliava J, Servant Y, Sommier L and Kahn O 1997 *Appl. Magn. Reson.* **12** 81
[8] Cantin C, Kliava J, Servant Y, Sommier L and Kahn O 1997 *Modern Applications of EPR/ESR* (Singapore: Springer) p 528
[9] Kliava J 1986 *Phys. Status Solidi* b **134** 411
[10] Shannon R D 1976 *Acta Crystallogr.* A **32** 751
[11] Cantin C 1997 *Thèse* Université Bordeaux I
[12] Vreugdenhil W, Haasnoot J G, Kahn O, Thuéry P and Reedijk J 1987 *J. Am. Chem. Soc.* **109** 5272